Liver INTERNATIONAL
OFFICIAL JOURNAL OF THE INTERNATIONAL ASSOCIATION FOR THE STUDY OF THE LIVER

Liver International ISSN 1478-3223

METABOLIC AND STEATOHEPATITIS

Strain dependence of diet-induced NASH and liver fibrosis in obese mice is linked to diabetes and inflammatory phenotype

Geoffrey C. Farrell[1], Auvro R. Mridha[1], Matthew M. Yeh[2], Todor Arsov[1], Derrick M. Van Rooyen[1], John Brooling[1], Tori Nguyen[1], Deborah Heydet[1], Viviane Delghingaro-Augusto[3], Christopher J. Nolan[3], Nicholas A. Shackel[4], Susan V. McLennan[5], Narci C. Teoh[1] and Claire Z. Larter[1]

1 Liver Research Group, Australian National University Medical School at The Canberra Hospital, Garran, ACT, Australia
2 Department of Pathology, University of Washington, Seattle, WA, USA
3 Department of Endocrinology, Canberra Hospital, Garran, ACT, Australia
4 Centenary Institute, Camperdown, NSW, Australia
5 Department of Endocrinology, Royal Prince Alfred Hospital, Camperdown, NSW, Australia

Keywords
cytokines – fibrosis – growth factors – Non-alcoholic steatohepatitis – strain difference

Abbreviations
ALT, alanine transaminase; CTGF, connective tissue growth factor; ELISA, enzyme-linked immunosorbent assay; GWAS, genome-wide association studies; H&E, haematoxylin and eosin; HCC, hepatocellular carcinoma; HF, high fat; IFN-γ, Interferon-γ; IL, Interleukin; MCP-1, monocyte chemoattractant protein-1; MMP, matrix metalloproteinase; NAFLD, non-alcoholic fatty liver disease; NAS, NAFLD activity score; NASH, non-alcoholic steatohepatitis; NOD, non-obese diabetic; PDGFα, platelet-derived growth factor α; PNPLA3, patatin-like phospholipase domain containing 3; SREBP-2, sterol regulatory element binding protein-2; T2D, Type 2 diabetes; TGF-β, transforming growth factor-β; TNF-α, tumour necrosis factor-α; WT, Wild type; α-SMA, α-Smooth muscle actin.

Correspondence
Professor Geoff Farrell, MD, FRACP
Liver Research Group, Australian National University Medical School
Level 5, Building 10 The Canberra Hospital
Yamba Drive, Garran, ACT 2605, Australia
Tel: +612 6244 2473
Fax: +612 6244 3235
e-mail: geoff.farrell@anu.edu.au

Received 8 May 2013
Accepted 6 September 2013

DOI:10.1111/liv.12335
Liver Int. 2014: 34: 1084–1093

Abstract

Background & Aims: Obese *Alms1* mutant (*foz/foz*) NOD.B10 mice develop diabetes and fibrotic NASH when fed high-fat(HF) diet. To establish whether diabetes or obesity is more closely associated with NASH fibrosis, we compared diabetic *foz/foz* C57BL6/J with non-diabetic *foz/foz* BALB/c mice. We also determined hepatic cytokines, growth factors and related profibrotic pathways. *Methods:* Male and female *foz/foz* BALB/c and C57BL6/J mice were fed HF or chow for 24 weeks before determining metabolic indices, liver injury, cytokines, growth factors, pathology/fibrosis and matrix deposition pathways. *Results:* All *foz/foz* mice were obese. Hepatomegaly, hyperinsulinemia, hyperglycaemia and hypoadiponectinaemia occurred only in *foz/foz* C57BL6/J mice, whereas *foz/foz* BALB/c formed more adipose. Serum ALT, steatosis, ballooning, liver inflammation and NAFLD activity score were worse in C57BL6/J mice. In HF-fed mice, fibrosis was severe in *foz/foz* C57BL6/J, appreciable in WT C57BL6/J, but absent in *foz/foz* BALB/c mice. Hepatic mRNA expression of TNF-α, IL-12, IL-4, IL-10 was increased (but not IFN-γ, IL-1β, IL-17A), and IL-4:IFN-γ ratio (indicating Th-2 predominance) was higher in HF-fed *foz/foz* C57BL6/J than BALB/c mice. In livers of HF-fed *foz/foz* C57BL6/J mice, TGF-β was unaltered but PDGFα and CTGF were increased in association with enhanced α-SMA, CD147and MMP activity. *Conclusions:* In mice with equivalent genetic/dietary obesity, NASH development is linked to strain differences in hyperinsulinaemia and hyperglycaemia inversely related to lipid partitioning between adipose and liver. Diabetes-mediated CTGF-regulation of MMPs as well as cytokines/growth factors (Th-2 cytokine predominant, PDGFα, not TGF-β) mobilized in the resultant hepatic necroinflammatory change may contribute to strain differences in NASH fibrosis.

Among patients with non-alcoholic fatty liver disease (NAFLD), 25–40% have type 2 diabetes (T2D), an additional 15–25% previously undiagnosed diabetes on oral glucose tolerance testing and/or a family history of T2D (1–3), and there is a three to four fold risk of developing diabetes within 3 years of NAFLD diagnosis.

Furthermore, insulin resistance and glucose intolerance are associated with a higher risk of fibrotic progression in NAFLD (4, 5). Experimentally, diabetes worsens fibrosis progression in dietary steatosis (6). While NAFLD is attributable to over-nutrition and under-activity (1, 2), not all over-weight/obese people develop NAFLD; an additional factor of individual susceptibility is required. Family studies, comparisons of NAFLD frequency between ethnic groups, and genome-wide association studies (GWAS) indicate that genetic predisposition underlines such individual susceptibility toNAFLD (7, 8), and also its severity (9). Some of these genetic polymorphisms influence bodily lipid partitioning and/or pathways of lipolysis or lipogenesis (*PNPLA3*) (7, 9). It also seems likely that genetic predisposition to diabetes predisposes to NAFLD, particularly its pathological more severe form of non-alcoholic steatohepatitis (NASH), and to NAFLD-related fibrotic progression (3).

In humans, rare single gene mutations profoundly alter appetite regulation, leading to obesity complicated by diabetes and NAFLD. Examples include defects in leptin, the leptin receptor and the Alström gene product (ALMS1). The latter causes Alström syndrome, a childhood obesity syndrome complicated by T2D, premature cardiovascular disease and cirrhosis (10, 11). Rodents with defective appetite regulation are widely used in diabetes and NAFLD research and include leptin-deficient *ob/ob* mice, and *db/db* mice and *fa/fa* rats with leptin receptor mutations. We have characterized *Alms1* mutant (*foz/foz*) NOD.B10 mice which likewise develop obesity, insulin resistance, hyperglycaemia/T2D, hypercholesterolaemia and hypertension (metabolic syndrome) (12–14). Feeding *foz/foz* mice high-fat (HF) diet containing 0.2% cholesterol accentuates metabolic complications that cause transition of steatosis to NASH with fibrosis (14, 15). *Alms1* locates to the anchoring site (basal body) of primary cilia (10, 13), and *foz/foz* mice exhibit at weaning a reduction in number of hypothalamic neurons that bear a primary cilium, in association with profound leptin resistance (13). The founder line of *foz/foz* mice was from a colony of non-obese diabetic (NOD) mice. If the only effect of the *Alms1* mutation is on appetite regulation, *foz/foz* mice of any strain should develop obesity, and it will be the strain response to obesity which determines the severity of resulting fatty liver disease. Those strains in which insulin resistance, metabolic syndrome and type 2 diabetes occur (as in human NASH) will develop NASH; those without insulin resistance and its metabolic complications will develop simple steatosis but not NASH. Conversely, if *Alms1* influences cellular factors operating in the pathogenesis of NASH, such as adipose differentiation, hepatic lipid handling and inflammatory recruitment, all *foz/foz* mice will develop the same pathological phenotype of NAFLD.

To test which of the above propositions is correct, we back-crossed the *Alms1* mutation onto C57BL6/J mice, which are known to develop diet-induced insulin resistance, and onto BALB/c mice, which are refractory to obesity-related diabetes (16). The finding of equivalent weight gain between strains confirms the central role of *Alms1* mutation on appetite dysregulation and resultant obesity. However, we found diametric differences in NASH fibrotic severity between HF-fed *foz/foz* C57BL6/J and BALB/c mice, which corresponded to marked differences in bodily fat distribution (adipose vs. liver), serum adiponectin, hyperinsulinaemia and glucose tolerance. Because of conflicting human data on the relative susceptibility of males and females to NAFLD, we also conducted the present studies on both male and female mice. We then explored whether the observed metabolic changes could influence fibrogenesis directly via connective tissue growth factor (CTGF), a protein responsive to diabetes and other metabolic factors. Finally, we assessed whether the Th-1 cytokine-modulated transforming growth factor (TGF)-β pathway, the Th-2 or Th-17 profibrotic pathways are involved in NAFLD-related fibrosis in these models.

Materials and methods

Animals and dietary regimens

Animal experiments were approved by the ANU Animal Ethics Committee. The *Alms1* 11-base pair truncating mutation (*foz*) was identified by 4% agarose gel electrophoresis of PCR products, as described (12). This allows heterozygotes, homozygous normal and *foz/foz* mice to be identified (12). Using heterozygous (*foz*/+) founder NOD.B10 mice (12), the *foz* mutation (i.e. *foz*/+ mice) was bred into BALB/c and C57BL6/J mice over 8 generations to yield *foz*/+ BALB/c or C57BL6/J mice that were, in turn, used to breed *foz/foz* mice of each strain. From 6 week age, groups (n = 4–10) of male or female *foz/foz* or littermate wild type (WT) C57BL6/J or BALB/c mice were fed either HF diet (23% fat, 45% carbohydrate, 20% protein, 0.19% cholesterol w/w; Specialty Feeds, Western Australia) or chow (Gordon's Speciality Stockfeed, New South Wales) for 24 weeks. Animals were fasted 4 h to determine blood glucose, anesthetized, blood, liver and adipose harvested. All animals tolerated the dietary regimen well and there was no mortality.

Assessment of liver injury and liver histology

Serum alanine aminotransferase (ALT) levels, histology of haematoxylin and eosin (H&E) stain liver sections [steatosis, ballooning, necroinflammatory and NAFLD activity score (NAS)] (14, 17), and Sirius red staining to determine fibrosis by image analysis quantification were as described (15).

Estimation of serum proteins and insulin resistance

Serum insulin (Millipore, Billerica, MA, USA), adiponectin, leptin, tumour necrosis factor-alpha (TNF)-α

and monocyte chemoattractant protein (MCP)-1 were measured by enzyme-linked immunosorbent assays (ELISA) (R&D Systems, Minneapolis, MN, USA). Insulin resistance (IR) was calculated from the product of fasting serum insulin and blood glucose (homeostatic assessment model, HOMA-IR) as follows: HOMA-IR = fasting blood glucose (mmol/L) × fasting serum insulin (mU/L) divided by 22.5.

Quantification of hepatic gene expression

For genes mentioned in results, semi-quantitative real-time PCR was performed (15) using primer sequences in Table S1.

Hepatic proteins

Expression of specific hepatic proteins was determined by Western immunoblot (antibody details provided on request) (14). Chemiluminescence images were captured, quantified, normalized to HSP-90 and presented relative to respective chow-fed WT strain controls.

Immunofluorescence staining

OCT-embedded liver sections were fixed with methanol/acetone and blocked with 3% BSA. Primary antibodies were applied, sections washed and fluorescent-labelled secondary antibodies added.

Matrix Metalloproteinase (MMP)

Total MMP activity was quantified by a commercial kit (Anaspec, Freemont, CA, USA). Gelatin zymography and *in situ* zymography were performed by established methods (18, 19). As negative control, MMP-specific activity was blocked with 10 mM 1,10-phenanthroline.

Statistical analyses

Data (mean ± SEM) were analysed by either one-way or two-way analysis of variance (ANOVA), followed by *post hoc* analysis using Bonferroni's multiple comparison test.

Results

Changes in body and tissue weights, and equivalent steatosis between strains

After 24 week, HF-fed *foz/foz* BALB/c and *foz/foz* C57BL6/J male mice were similarly obese (Fig. 1A), with <15% difference in body weight between groups by diet, genotype and strain. Similar data were noted in females (Fig. S1A). However, bodily fat distribution differed dramatically between the 2 strains of obese mice. White adipose tissue (WAT) expansion (as peri-epididymal fat weight) was >50% greater in *foz/foz* BALB/c than *foz/foz* C57BL6/J males (Fig. 1B), and >three-fold (periovarian WAT) in females (Fig. S1B); there were similar (and proportional) changes in subcutaneous WAT (data not shown). Conversely, hepatomegaly occurred in *foz/foz* C57BL6/J mice (fed HF or chow) as well as in HF-fed male WT C57BL6/J (Fig. 1C; Fig. S1C). The hepatomegaly observed in *foz/foz* C57BL6/J mice was attributable to steatosis, as indicated by the greasy pale macroscopic appearance (not shown) and grade 3 steatosis score (Fig. 1D; Fig. S1D). As reported by others (6), we also observed severe steatosis in HF-fed WT C57BL6/J mice, and it was conspicuous (albeit not causing hepatomegaly) in *foz/foz* BALB/c mice (Fig. 1D; Fig. S1D).

Metabolic and inflammatory complications of obesity occur in C57BL6/J but not BALB/c mice

A striking feature of our earlier work in HF-fed *foz/foz* NOD.B10 mice is hyperinsulinaemia and early onset diabetes (12, 14, 15). As shown in Fig. 1E (Supplementary Fig. SE for females), HF feeding cause minimal (if any) increases in fasting serum insulin in WT C57BL6/J or BALB/c mice of either strain. On the other hand, *foz/foz* C57BL6/J mice fed chow or HF diet, but not *foz/foz* BALB/c mice, exhibited five- to 20-fold-increases in fasting serum insulin compared with corresponding WT mice (Fig. 1E; Fig. S1E). The metabolic significance of hyperinsulinaemia in *foz/foz* C57BL6/J mice was evident by fasting hyperglycaemia, which exceeded 8 mmol/L (diabetes) in these 2 groups (Fig. 1F; Fig. S1F) reflecting insulin resistance as indicated by the increase in HOMA-IR (Fig. 1G; Fig. S1G). HF-fed *foz/foz* C57BL6/J (and also chow-fed *foz/foz* C57BL6/J female) but not HF-fed *foz/foz* BALB/c mice also develop hypercholesterolaemia (Fig. 1H; Fig. S1H). Consistent with these metabolic complications of obesity, both chow and HF-fed *foz/foz* C57BL6/J mice exhibited significant falls in serum adiponectin compared with *foz/foz* BALB/c counterparts (Fig. 1I; Fig. S1I). Conversely, both strains of *foz/foz* mice showed the increase in serum leptin expected direct proportional to body weight (data not shown).

NAFLD is more severe in HF-fed foz/foz C57BL6/J than BALB/c mice

In male mice, serum ALT exceeded 300 U/L in HF-fed *foz/foz* C57BL6/J mice compared to ca. 100U/L in HF-fed *foz/foz* BALB/c, chow-fed *foz/foz* C57BL6/J and HF-fed WT C57BL6/J mice (Fig. 2A). A similar and more pronounced pattern of ALT changes was observed in females (Fig. S2A). The severity of hepatocellular ballooning (Fig. 2B) and necroinflammatory scores (Fig. 2C) were broadly similar to ALT in male mice, but ballooning and necroinflammatory change were also evident in female HF-fed *foz/foz* BALB/c mice (Fig. S2B, 2C). The NAFLD Activity Score (NAS) was 5–6 in HF-fed *foz/foz* C57BL6/J male and female mice (Fig. 2D; Fig. S2D), and 4–5 in HF-fed WT C57BL6/J mice, and in female, but not male HF-fed *foz/foz* BALB/c mice,

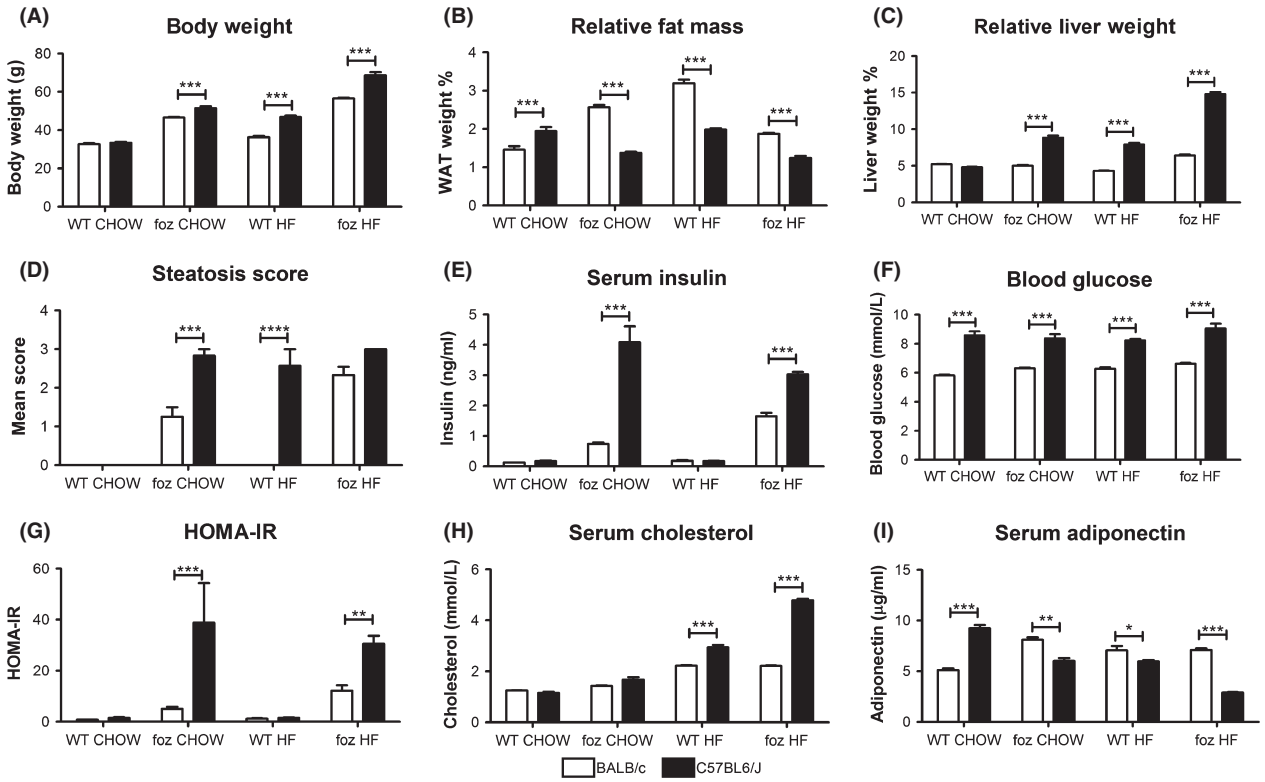

Fig. 1. Body weight, tissue weights, steatosis and metabolic complications of obesity in male *foz/foz* and WT C57BL6/J and BALB/c mice. (A) After 24 weeks of HF feeding WT and *foz/foz* C57BL6/J mice weighed slightly more than corresponding BALB/c mice. (B) In *foz/foz* and HF-fed WT mice, WAT mass was greater in BALB/c than C57BL6/J, but (C) hepatomegaly occurred only in HF-fed *foz/foz* C57BL6/J mice. (D) Steatosis was observed in both *foz/foz* strains (irrespective of diet) and HF-fed WT C57BL6/J mice. (E) Serum insulin increased markedly in *foz/foz* C57BL6/J mice, and (F) fasting blood glucose was higher in C57BL6/J mice compared to BALB/c counterparts. (G) HOMA-IR increased in C57BL6/J but not BALB/c mice. (H) Hypercholesterolaemia occurred in HF-fed *foz/foz* C57BL6/J mice, but not in BALB/c counterparts. (I) Serum adiponectin levels fell in chow and HF-fed *foz/foz* C57BL6/J mice compared to BALB/c counterparts. Data are mean ± SEM, $*P \leq 0.05$, $**P \leq 0.01$, $***P \leq 0.001$ and $****P \leq 0.0001$, by two-way ANOVA with Bonferroni's test (same animals as in Table 1).

corresponding to the presence of definite or borderline NASH in these groups, as appraised by global assessment of liver pathology (Table 1, Fig. 2G; Fig. S2G). While the pattern of elevated serum MCP-1 levels resembled the NAS (Fig. 2E vs. Fig. 2D), serum TNF-α levels were highly variable, and below detection in many animals in all groups (not shown).

Liver fibrosis occurs in C57BL6/J but not in BALB/c mice

Appreciable fibrosis (Sirius red staining) occurred only in HF-fed *foz/foz* or WT C57BL6/J mice of either gender (Fig. 2F, 2H; Fig. S2F, 2H). It was most severe in HF-fed *foz/foz* C57BL6/J mice (both genders), but absent in HF-fed *foz/foz* (and WT) BALB/c mice (Fig. 2H; Fig. S2H). The differences between groups are most evident by Sirius red densitometry (Fig. 2F; Fig. S2F).

Hepatic cytokine and growth factor expression

BALB/c mice are not inherently refractory to hepatic fibrosis. Actually, for some forms of liver injury they are particularly prone to fibrotic responses and this has been attributed to a Th2-weighted cytokine response in this strain, particularly IL-4. In the present studies, only TNF-α (Fig. 3A) and IL-12 (Fig. 3B) transcripts among Th-1 cytokines were increased in livers of HF-fed WT and *foz/foz* C57BL6/J mice compared with BALB/c counterparts, with no change in interferon (IFN)-γ (Fig. 3C) or IL-1β (Fig. 3D) or in Th-17-related IL-17A (Fig. 3E) and IL-13 (data not shown). On the other hand, there was an important increase in IL-4 mRNA in HF-fed *foz/foz* C57BL6/J vs. BALB/c mice (Fig. 3G), and broadly similar changes in IL-10 mRNA (Fig. 3F). In addition, HF-fed *foz/foz* C57BL6/J mice showed an increase in the ratio of IL-4 to IFN-γ mRNA, which was not altered in BALB/c mice (Fig. 3H).

The key profibrotic factor TGF-β is partly regulated by TNF-α; despite a variable increase in hepatic TNF-α mRNA (Fig. 3A), hepatic TGF-β expression appeared similar in all groups (Fig. 3I, M). Conversely, platelet-derived growth factor (PDGF)-α expression increased in all C57BL6/J mice with NAFLD fibrosis, but not in corresponding BALB/c mice (Fig. 3J, M). CTGF is

Table 1. Liver histology of male mice revealed NASH in HF-fed *foz* C57BL6/J, but not BALB/c mice

Strain	Group	*n*	Normal	NAFLD not NASH	Borderline NASH	Definite NASH
BALB/c	WT CHOW	4	4 (100%)	0	0	0
	foz CHOW	8	7 (87.5%)	1 (12.5%)	0	0
	WT HF	4	4 (100%)	0	0	0
	foz HF	6	2 (33%)	4 (67%)	0	0
C57BL6/J	WT CHOW	4	4 (100%)	0	0	0
	foz CHOW	6	0	0	2 (33)%	4 (67)%
	WT HF	7	1 (14%)	2 (28.5)%	2 (28.5)%	2 (28.5)%
	foz HF	4	0	0	1 (25%)	3 (75%)

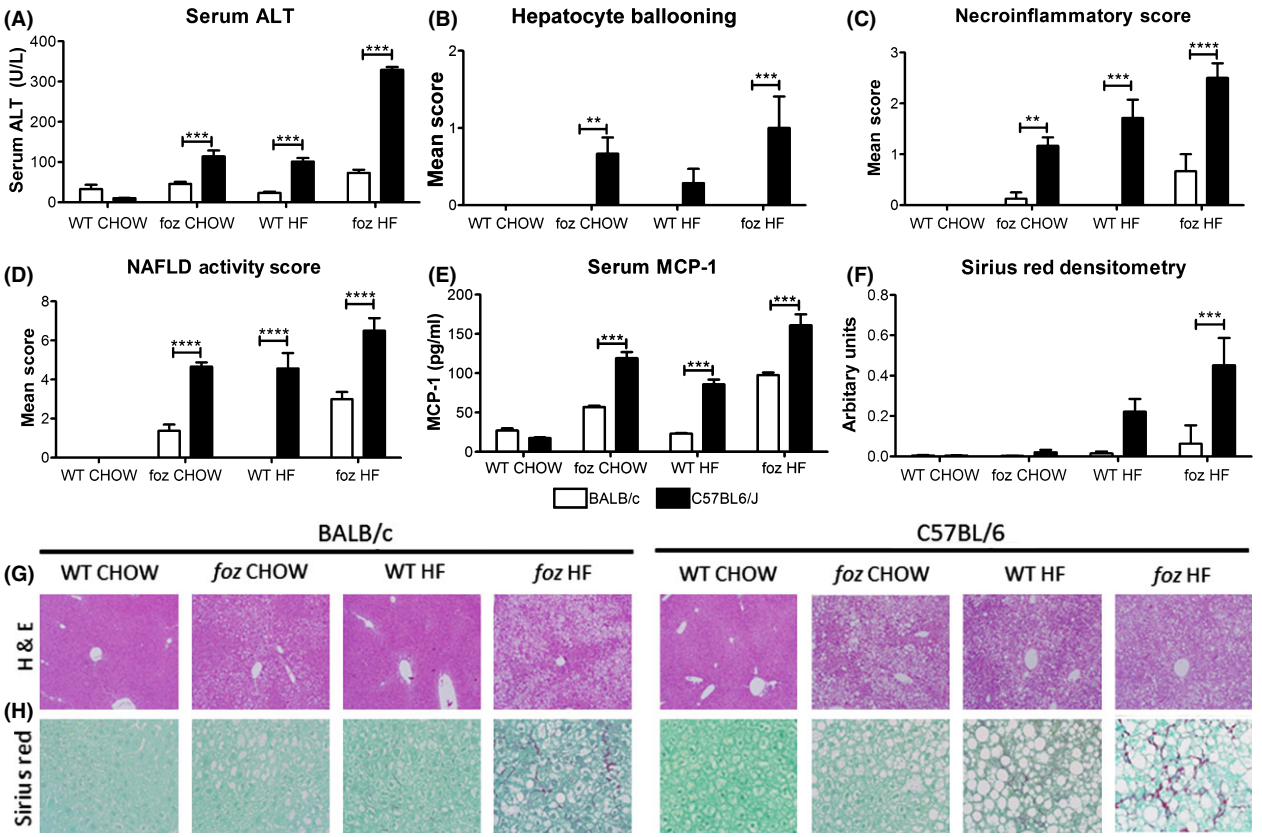

Fig. 2. Steatohepatitis occurs in both strains of HF-fed *foz/foz* male mice, whereas liver fibrosis occurs in HF-fed *foz/foz* C57BL6/J but not in BALB/c mice. (A) Serum ALT was higher in HF-fed *foz/foz* C57BL6/J mice compared to other groups. (B) Hepatocyte ballooning, (C) necroinflammatory changes, and (D) NAFLD activity score (NAS) were all increased in HF-fed WT and *foz/foz* C57BL6/J mice and in HF-fed *foz/foz* BALB/c mice. (E) Increases in serum MCP-1 were similar to NAS. (F) Densitometry analysis of Sirius red stain was highest in HF-fed *foz/foz* C57BL6/J. Representative images of (G) liver histology by haematoxylin and eosin (H&E) stain and (H) collagen deposition by Sirius red stain. Data are mean ± SEM $*P \leq 0.05$, $**P \leq 0.01$, $***P \leq 0.001$, $***P \leq 0.0001$ and $****P < 0.0001$, by two-way ANOVA with Bonferroni's test (same animals as in Table 1).

regulated by glucose and insulin-like growth factors; values increased two-fold in HF-fed *foz/foz* C57BL6/J livers (Fig. 3K, B ($P < 0.001$), and this was strongly associated with Sirius red densitometry (Fig. 2F), enhanced α-smooth muscle actin (SMA) (Fig. 3L, M), and collagen-1α mRNA (not shown).

CD147-mediated effects on MMP activity in foz/foz C57BL6/J mice with fibrosis

In other work, some of us have shown that CTGF activation is associated with fibrotic progression in a nutritional model of steatohepatitis (HF-fed WT C57BL6/J

Liver International (2014)

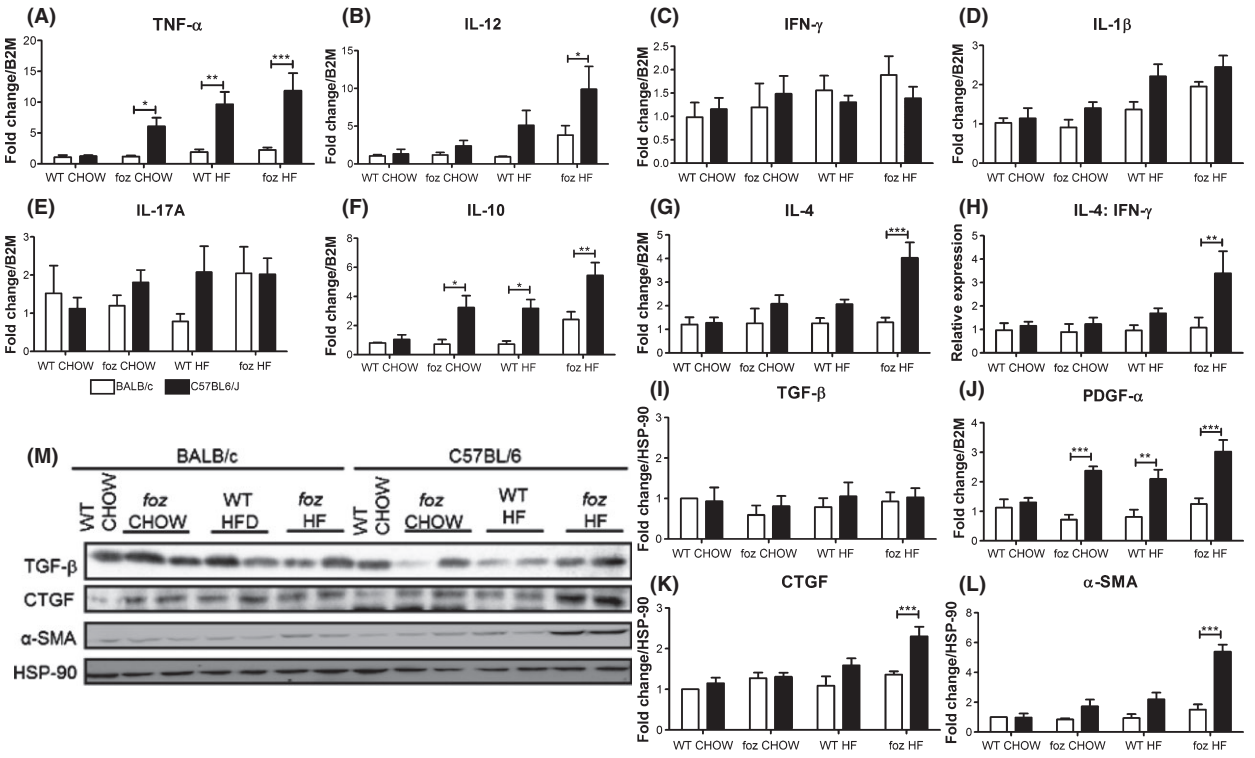

Fig. 3. Selective changes in Th-1 and Th-2 cytokines, PDGFα, CTGF and α-SMA expression in HF-fed *foz/foz* C57BL6/J mice vs. corresponding BALB/c mice. Hepatic mRNA expression of Th-1 cytokines (A) TNF-α and (B) IL-12 were increased in HF-fed *foz/foz* C57BL6/J compared with BALB/c mice, but (C) IFN-γ and (D) IL-1β were unaltered. Th-17 related (E) IL-17A was unaltered across all groups/strains. Th-2 cytokines (F) IL-10 and (G) IL-4 were markedly increased in HF-fed *foz/foz* C57BL6/J compared to BALB/c mice, so that (H) the IL4: IFN-γ was increased HF-fed *foz/foz* C57BL6/J, compared to BALB/c mice. (I) TGF-β levels were unaltered, but (J) PDGFα, (K) CTGF, and (L) α-SMA expression were significantly higher in HF-fed *foz/foz* C57BL6/J than in BALB/c mice. (M) Representative Western Blots are shown for TGF-β, CTGF, α-SMA and HSP-90 (as loading control). Data are mean ± SEM $*P \leq 0.05$, $**P \leq 0.01$ and $***P \leq 0.001$, by two-way ANOVA with Bonferroni's test (same animals as in Table 1).

mice) when streptozotocin was administered to cause diabetes (6). If diabetes is responsible for CTGF-induced liver fibrosis in NASH, we would expect that the pronounced increase in CTGF observed in HF-fed *foz/foz* C57BL6/J (but not in similarly fed *foz/foz* BALB/c mice) (Fig, 3K, 3M) would be associated with congruent profibrotic pathways. CD147 is secreted by hepatocytes and regulates MMP activity (20). In this study, we showed that increased CTGF expression in *foz/foz* C57BL/6 mice is associated with increased expression of CD147 around hepatocytes (Fig. 4A), and we confirmed a close relationship between CD147 expression and *in situ* MMP activity (Fig. 4B). The basis of such MMP activation was revealed by the anticipated effects of increased CD147 (Fig. 4C, D) in HF-fed *foz/foz* C57BL6/J mice, including increased total MMP activity (Fig. 4E), and expression of MMP-2 and -9 (Figs. 4F, 4G and 4H).

Discussion

The severity of NAFLD is worse in diabetes (1–4), with more progression to NASH, cirrhosis and HCC, while the possibility that "diabetes genes" separately influence NASH fibrosis has been raised by observations in families (3). In earlier study in *foz/foz* (*Alms1* mutant) mice, we employed the NOD.B10 strain, which is genetically prone to diabetes. In such animals, serum insulin reaches very high levels and we have shown that this drives SREBP-2-mediated dysregulation of hepatocyte cholesterol metabolism (2, 12) that is central to the lipotoxic pathogenesis of NASH (15, 18). In the same model, we have also shown that dietary (21) and pharmacological strategies that improve insulin sensitivity, thereby lowering serum insulin, improve NAFLD severity and liver fibrosis (22–24).

The first major finding of this study was that NAFLD is more severe, with higher NAS and clear evidence of NASH, in HF-fed *foz/foz* C57BL6/J mice than in corresponding *foz/foz* BALB/c mice. Like NOD.B10 mice, *foz/foz* C57BL/6 mice develop insulin resistance with hyperinsulinaemia and diabetes whereas *foz/foz* BALB/c mice do not. The differences were most clear-cut in males as female *foz/foz* BALB/c mice developed some ballooning and necroinflammatory change as well as steatosis. However, an even more important and highly

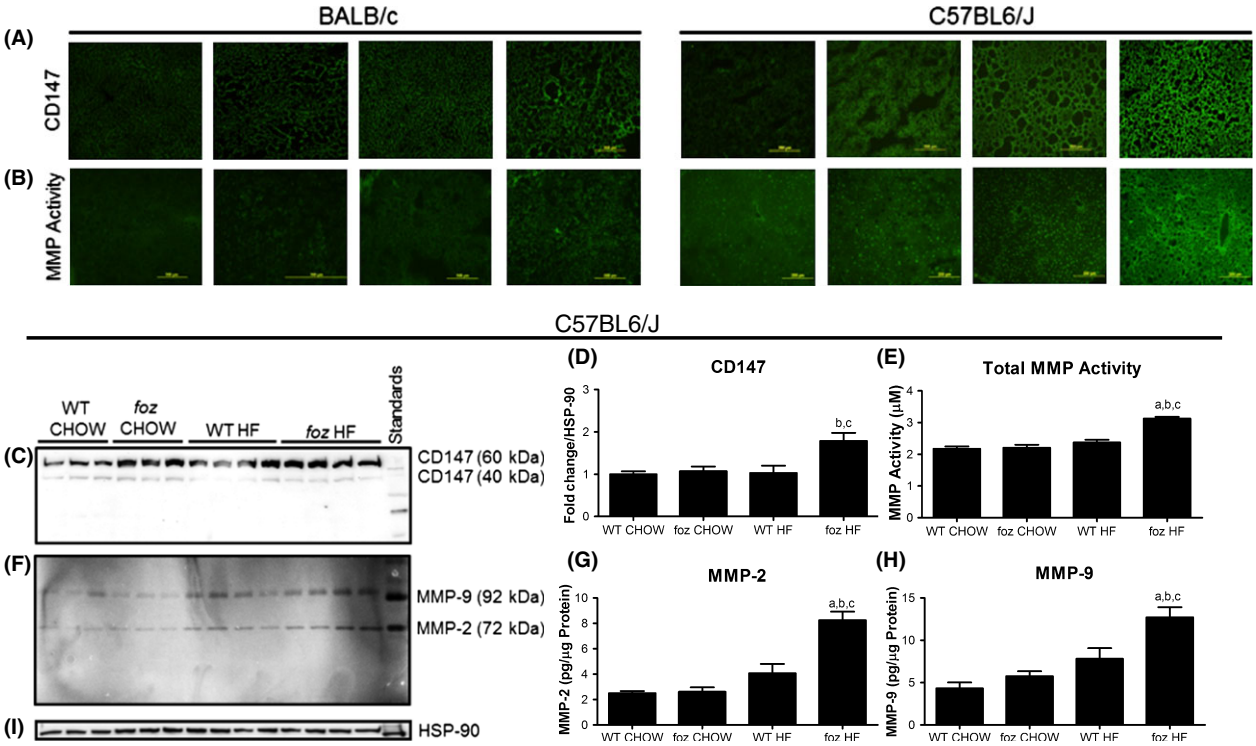

Fig. 4. Hepatic expression of CD147 and MMPs were increased in HF-fed male *foz/foz* C57BL6/J but not BALB/c mice. (A) Immunofluorescent staining of CD147 increased around hepatocytes in HF-fed *foz/foz* C57BL6/J, but not BALB/c mice, (B) increased MMP activity by *in situ* zymography in HF-fed *foz/foz* C57BL6/J mice, (C and D) CD147 expression increased in HF-fed *foz/foz* C57BL6/J mice. Similar patterns for (E) total MMP activity, (F, G and H) MMPs-2 and -9. (I) HSP-90 loading control. Data are mean ± SEM $P \leq 0.05$ significantly different from [a]WT CHOW, [b]*foz* CHOW, [c]WT HFD, by one-way ANOVA with Bonferroni's test (same animals as in Table 1).

reproducible difference was that *foz/foz* C57BL6/J develop substantial NAFLD-related fibrosis but *foz/foz* BALB/c mice do not. It should be noted that BALB/c mice are not refractory to hepatic fibrosis caused by non-metabolic factors, such as toxins (25, 26) and schistosomiasis (27), in fact BALB/c mice are actually the most susceptible mouse strain to CCl_4 injury and fibrosis (28). Furthermore, C57BL6/J mice *without* the *foz/foz* defect also develop hepatic fibrosis in the presence of NASH, as shown by some of us earlier (6) and confirmed here. It is therefore clear that the observed strain-dependent difference in fibrotic severity of NAFLD is not because of a direct effect of the *Alms1* mutation in mediation of liver fibrosis. Instead, it must be because of the differing metabolic context (insulin resistance, diabetes) and/or the more severe necroinflammatory response to liver injury caused by disordered bodily lipid partitioning.

Strain-specific differences in susceptibility to diet-induced NAFLD/NASH are well known. Among 10 different mouse strains, hepatic triglyceride levels are actually highest in BALB/c, moderate in C57BL6/J and lowest in SWR strains (29). In the present experiments, steatosis was similar in *foz/foz* C57BL6/J and BALB/c mice (both genders), but hyperinsulinaemia, hyperglycaemia and hypoadiponectinaemia were conspicuous only in C57BL6/J, not in BALB/c mice. BALB/c mice appear to form WAT more efficiently than C57BL6/J (or NOD.B10) mice (2, 15), and this may be a protective mechanism against hepatic accumulation of toxic lipid molecules that cause liver injury in NASH and which contribute to insulin resistance. However, there did not appear to be strain-specific differences in patterns of adipose distribution, such as the relative limitation of subcutaneous adipose with expansion of visceral adipose that is found in humans with NASH (1, 2).

The second important finding of this study is that the appetite defect in *foz/foz* mice, recently attributed to a defect in hypothalamic neuronal cilial stability (13), results in excessive weight gain independent of background strain and minimally influenced by gender. Thus, at the end of the 24-week feeding experiments, chow or HF-fed male *foz/foz* C57BL6/J mice weighed only slightly more than their BALB/c counterparts, while *foz/foz* C57BL6/J and BALB/c females were of similar weight. Despite this, *foz/foz* C57BL6/J mice develop hyperinsulinaemia and diabetes, whereas the similarly obese HF-fed *foz/foz* BALB/c mice do not. Thus, genetic differences between the C57BL6/J and BALB/c strains determine onset of insulin resistance and diabetes as

obesity occurs. The strain-dependent fall in serum adiponectin is further evidence that metabolic disease in obese mice depends on variables other than the *Alms1* mutation which leads to obesity.

In addition to the metabolic differences, it is possible that the observed strain differences in NAFLD-related fibrogenesis could be partly because of differences in the necroinflammatory activity of NASH, because serum ALT levels were higher in HF-fed *foz/foz* C57BL6/J than corresponding BALB/c mice, and hepatomegaly was more pronounced. Inflammation can involve platelet activation, and it is noteworthy that the profibrogenic PDGFα was expressed only in C57BL6/J livers with NAFLD. It is also possible that the immunophenotype of liver inflammation differs between C57BL6/J and BALB/c mice with NAFLD (30). In the present studies, circulating levels of the macrophage chemokine, MCP-1, implicated in hepatic fibrogenesis (31) were increased in C57BL6/J mice with NASH compared with their BALB/c counterparts, while hepatic TNF-α mRNA levels (but not serum levels) followed a similar strain-selective pattern. While hepatic expression of several cytokines increased in C57BL6/J mice with NASH (TNF-α, IL-12, IL-4, IL-10), others were not increased (IFN-γ, IL-1β, IL-17A, IL-13). Furthermore, the balance reflected by the IL-4: IFN- γ ratio was Th-2 weighed, not Th-1 or Th-17. This has previously been noted to indicate a higher probability of liver fibrosis (30). On the other hand, it is notable that hepatic expression of the profibrogenic growth factor TGF-β, which is responsive to Th-1 cytokines, did not differ between C57BL6/J and BALB/c mice.

In addition to the changes in PDGFα and Th-2 weighted cytokines, we consider that a cogent explanation for fibrotic differences between C57BL6/J and BALB/c mice with NAFLD is that the divergent metabolic differences between strains effects CTGF expression. Hyperglycaemia, insulin-like growth factors and integrin interactions are among the factors known to increase CTGF expression (32). CTGF regulates fibrosis in skin, heart, kidney and lungs, while hepatic (and serum) CTGF expression increases in NASH (33). The low levels of CTGF expressed by hepatocytes are increased by liver injury, and increases in serum and liver CTGF levels have been reported in several models of liver fibrosis (34, 35). CTGF activates survival pathways in hepatic stellate cells (HSCs) and induces expression of α-SMA and type 1 collagen (35), strongly supporting a role for CTGF in hepatic fibrogenesis. It was previously thought that CGTF stimulation depended on TGF-β, but TGF-β-independent regulatory pathways have now been identified (36, 37). For instance, MMPs bind a CTGF enhancer element to increase CTGF expression (36). In this respect, it is possible that CD147, a plasma membrane glycoprotein (20) which we found activated in HF-fed *foz/foz* C57BL6/J but not *foz/foz* BALB/c mice with NASH, may play a role shifting the balance towards MMP production and activation.

In summary, all strains of *Alms1* mutant (*foz/foz*) mice develop equivalent obesity, but there are striking strain-dependent responses to obesity. BALB/c mice appear to form WAT more efficiently than C57BL6/J (or NOD.B10) mice (2, 15) and this may protect them from the metabolic complications of obesity, such as insulin resistance and NASH. Thus, while *foz/foz* C57BL6/J develop hyperinsulinaemia, diabetes, hypercholesterolaemia, hypoadiponectinaemia and severe NAFLD, *foz/foz* BALB/c mice fed the same HF diet are metabolically normal and have less severe NAFLD. The strain-dependent metabolic differences observed between C57BL6/J and BALB/c mice influence development of steatohepatitis, more so in male than female mice. There were also differences in circulating MCP-1, hepatic PDGFα expression, and Th-2 weighted hepatic cytokine expression related to differences in severity of liver inflammation between the two strains. However, Th-1 regulated TGF-β failed to explain the major differences observed in NASH fibrosis, which was severe in HF-fed *foz/foz* C57BL6/J mice, moderate in their chow-fed *foz/foz* or HF-fed WT counterparts, and virtually absent in HF-fed *foz/foz* BALB/c mice. Conversely, hyperinsulinaemia and hyperglycaemia were associated with increased hepatic expression of CTGF that interacts with CD147-mediated regulation of MMP activity via MMP-2 and -9. These important differences between mouse strains in NASH fibrosis that are seemingly related to metabolic factors provide an experimental model to consider factors which counter insulin resistance, such as moderately vigorous regular exercise (38) as well as the pharmacological agents studied earlier (22–24), as approaches to prevent liver fibrosis in NASH.

Acknowledgements

Financial support: Supported by NHMRC project grants 585411, 102818 and 1042288. CZL was supported by an NHMRC Australian Post-doctoral Training Fellowship (525473), and DVR by NHMRC Scholarship 585539.

Conflicts of interest: The authors have no conflicts to disclose.

References

1. Cusi K. Role of obesity and lipotoxicity in the development of nonalcoholic steatohepatitis: Pathophysiology and clinical implications. *Gastroenterology* 2012; **142**: 711–25.
2. Larter CZ, Chitturi S, Heydet D, Farrell GC. A fresh look at NASH pathogenesis. Part 1: the metabolic movers. *J Gastroenterol Hepatol* 2010; **25**: 672–90.
3. Loomba R, Abraham M, Unalp A, *et al.* Association between diabetes, family history of diabetes, and risk of nonalcoholic steatohepatitis and fibrosis. *Hepatology* 2012; **56**: 943–51.
4. Angulo P, Hui JM, Marchesini G, *et al.* The NAFLD fibrosis score: A noninvasive system that identifies liver fibrosis in patients with NAFLD. *Hepatology* 2007; **45**: 846–54.
5. Argo CK, Northup PG, Al-Osaimi AMS, Caldwell SH. Systematic review of risk factors for fibrosis progres-

sion in non-alcoholic steatohepatitis. *J Hepatol* 2009; **51**: 371–9.
6. Lo L, Mclennan SV, Williams PF, *et al.* Diabetes is a progression factor for hepatic fibrosis in a high fat fed mouse obesity model of non-alcoholic steatohepatitis. *J Hepatol* 2011; **55**: 435–44.
7. Romeo S, Kozlitina J, Xing C, *et al.* Genetic variation in PNPLA3 confers susceptibility to nonalcoholic fatty liver disease. *Nat Genet* 2008; **40**: 1461–5.
8. Valenti L, Al-Serri A, Daly AK, *et al.* Homozygosity for the patatin-like phospholipase-3/adiponutrin I148M polymorphism influences liver fibrosis in patients with nonalcoholic fatty liver disease. *Hepatology* 2010; **51**: 1209–17.
9. Chalasani N, Guo X, Loomba R, *et al.* Genome-wide association study identifies variants associated with histologic features of nonalcoholic fatty liver disease. *Gastroenterology* 2010; **139**: 1567–76.
10. Collin GB, Marshall JD, Ikeda A, *et al.* Mutations in ALMS1 cause obesity, type 2 diabetes and neurosensory degeneration in Alstrom syndrome. *Nat Genet* 2002; **31**: 74–8.
11. Marshall JD, Beck S, Maffei P, Naggert JK. Alstrom Syndrome. *Eur J Hum Genet* 2007; **15**: 1193–202.
12. Arsov T, Silva DG, O'bryan MK, *et al.* Fat Aussie—A new Alström syndrome mouse showing a critical role for ALMS1 in obesity, diabetes, and spermatogenesis. *Mol Endocrinol* 2006; **20**: 1610–22.
13. Heydet D, Chen LX, Larter CZ, *et al.* A truncating mutation of Alms1 reduces the number of hypothalamic neuronal cilia in obese mice. *Dev Neurobiol* 2012; **73**: 1–13.
14. Larter CZ, Yeh MM, Van Rooyen DM, *et al.* Roles of adipose restriction and metabolic factors in progression of steatosis to steatohepatitis in obese, diabetic mice. *J Gastroenterol Hepatol* 2009; **24**: 1658–68.
15. Van Rooyen DM, Larter CZ, Haigh WG, *et al.* Hepatic free cholesterol accumulates in obese, diabetic mice and causes nonalcoholic steatohepatitis. *Gastroenterology* 2011; **141**: 1393–403.
16. Ozcan U, Cao Q, Yilmaz E, *et al.* Endoplasmic reticulum stress links obesity, insulin action, and type 2 diabetes. *Science* 2004; **306**: 457–61.
17. Kleiner DE, Brunt EM, Van Natta M, *et al.* Design and validation of a histological scoring system for nonalcoholic fatty liver disease. *Hepatology* 2005; **41**: 1313–21.
18. Min D, Lyons JG, Jia J, Lo L, Mclennan SV. 2-Methoxy-2,4-diphenyl-3(2H)-furanone-labeled gelatin zymography and reverse zymography: A rapid real-time method for quantification of matrix metalloproteinases-2 and -9 and tissue inhibitors of metalloproteinases. *Electrophoresis* 2006; **27**: 357–64.
19. Mook OR, Van Overbeek C, Ackema EG, Van Maldegem F, Frederiks WM. In situ localization of gelatinolytic activity in the extracellular matrix of metastases of colon cancer in rat liver using quenched fluorogenic DQ-gelatin. *J Histochem Cytochem* 2003; **51**: 821–9.
20. Biswas C, Zhang Y, Decastro R, *et al.* The human tumor cell-derived collagenase stimulatory factor (renamed EMMPRIN) is a member of the immunoglobulin superfamily. *Cancer Res* 1995; **55**: 434–9.
21. Larter CZ, Yeh MM, Haigh WG, *et al.* Dietary modification dampens liver inflammation and fibrosis in obesity-related fatty liver disease. *Obesity* 2013; **21**: 1189–99.
22. Bell-Anderson KS, Aouad L, Williams H, *et al.* Coordinated improvement in glucose tolerance, liver steatosis and obesity-associated inflammation by cannabinoid 1 receptor antagonism in fat Aussie mice. *Int J Obes* 2011; **35**: 1539–48.
23. Larter CZ, Yeh MM, Van Rooyen DM, *et al.* Peroxisome proliferator-activated receptor-α agonist, Wy 14,643, improves metabolic indices, steatosis and ballooning in diabetic mice with non-alcoholic steatohepatitis. *J Gastroenterol Hepatol* 2012; **27**: 341–50.
24. Van Rooyen DM, Gan LT, Yeh MM, *et al.* Pharmacological cholesterol lowering reverses fibrotic NASH in obese, diabetic mice with metabolic syndrome. *J Hepatol* 2013; **59**: 144–52.
25. Bhathal PS, Rose NR, Macay IR, Whittingham S. Strain differences in mice in carbon tetrachloride-induced injury. *Br J Exp Pathol* 1983; **64**: 524.
26. Wang M-E, Chen Y-C, Chen IS, *et al.* Curcumin protects against thioacetamide-induced hepatic fibrosis by attenuating the inflammatory response and inducing apoptosis of damaged hepatocytes. *J Nutri Biochem* 2012; **23**: 1352–66.
27. Van De Vijver KK, Colpaert CG, Jacobs W, *et al.* The host's genetic background determines the extent of angiogenesis induced by schistosome egg antigens. *Acta Trop* 2006; **99**: 243–51.
28. Hillebrandt S, Goos C, Matern S, Lammert F. Genome-wide analysis of hepatic fibrosis in inbred mice identifies the susceptibility locus Hfib1 on chromosome 15. *Gastroenterology* 2002; **123**: 2041–51.
29. Lin X, Yue P, Chen Z, Schonfeld G. Hepatic triglyceride contents are genetically determined in mice: results of a strain survey. *Am J Phisiol- Gastro Liv Phisiol* 2005; **288**: G1179–89.
30. Shi Z, Wakil AE, Rockey DC. Strain-specific differences in mouse hepatic wound healing are mediated by divergent T helper cytokine responses. *Proc Natl Acad Sci* 1997; **94**: 10663–8.
31. Marra F, Romanelli RG, Giannini C, *et al.* Monocyte chemotactic protein-1 as a chemoattractant for human hepatic stellate cells. *Hepatology* 1999; **29**: 140–8.
32. Paradis V, Perlemuter G, Bonvoust F, *et al.* High glucose and hyperinsulinemia stimulate connective tissue growth factor expression: A potential mechanism involved in progression to fibrosis in nonalcoholic steatohepatitis. *Hepatology* 2001; **34**: 738–44.
33. Rachfal AW, Brigstock DR. Connective tissue growth factor (CTGF/CCN2) in hepatic fibrosis. *Hepatol Res* 2003; **26**: 1–9.
34. Kodama T, Takehara T, Hikita H, *et al.* Increases in p53 expression induce CTGF synthesis by mouse and human hepatocytes and result in liver fibrosis in mice. *J Clin Invest* 2011; **121**: 3343–56.
35. Paradis V, Dargere D, Bonvoust F, *et al.* Effects and regulation of connective tissue growth factor on hepatic stellate cells. *Lab Invest* 2002; **82**: 767–74.
36. Eguchi T, Kubota S, Kawata K, *et al.* Novel transcription-factor-like function of human matrix metalloproteinase 3 regulating the CTGF/CCN2 gene. *Mol Cell Biol* 2008; **28**: 2391–413.
37. Gressner OA, Lahme B, Demirci I, Gressner AM, Weiskirchen R. Differential effects of TGF-β on connective tissue growth factor (CTGF/CCN2) expression in hepatic stellate cells and hepatocytes. *J Hepatol* 2007; **47**: 699–710.

38. Kistler KD, Brunt EM, Clark JM, *et al.* Physical Activity Recommendations, Exercise Intensity, and Histological Severity of Nonalcoholic Fatty Liver Disease. *Am J Gastroenterol* 2011; **106**: 460–8.

Supporting information

Additional Supporting Information may be found in the online version of this article:

Table S1. List of primers sequences.

Fig. S1. Body weight, tissue weights, steatosis and metabolic determinants of obesity in female foz/foz and WT C57BL6/J and BALB/c mice.

Fig. S2. In female mice steatohepatitis occurs in both strains of HF-fed foz/foz mice, whereas liver fibrosis occurs in HF-fed foz/foz C57BL6/J, but not in BALB/c mice.

Fig. S3. Method for back-crossing Alms1 (foz) mutation from founder NOD.B10 strain onto BALB/c background (method for C57BL6/J was identical).

Fig. S4. Intraperitoneal glucose tolerance testing (IPGTT) of wildtype (WT) C57BL/6 mice fed 26–30 weeks either chow or the same high-fat diet (HF), as used in this study.

Fig. S5. Intraperitoneal glucose tolerance testing of foz/foz and WT BALB/c mice fed the same high-fat diet (HF), as used in this study for 8 weeks (the mice are 11 weeks of age).